



# Fibroblast Activation Protein Specific Optical Imaging in Non-Small Cell Lung Cancer

Layla Mathieson<sup>1,2</sup>, Richard A. O'Connor<sup>1,2</sup>, Hazel Stewart<sup>2</sup>, Paige Shaw<sup>3</sup>, Kevin Dhaliwal<sup>1,2</sup>, Gareth O. S. Williams<sup>2</sup>, Alicia Megia-Fernandez<sup>3</sup> and Ahsan R. Akram<sup>1,2,4\*</sup>

<sup>1</sup> Centre for Inflammation Research, Queen's Medical Research Institute, University of Edinburgh, Edinburgh, United Kingdom, <sup>2</sup> Translational Healthcare Technologies Group, Centre for Inflammation Research, Queen's Medical Research Institute, University of Edinburgh, Edinburgh, United Kingdom, <sup>3</sup> EaStCHEM, The University of Edinburgh School of Chemistry, Edinburgh, United Kingdom, <sup>4</sup> Cancer Research UK Edinburgh Centre, Institute of Genetics and Cancer, The University of Edinburgh, Edinburgh, United Kingdom

## OPEN ACCESS

### Edited by:

Paul Takam Kamga,  
Université de Versailles Saint-Quentin-  
en-Yvelines, France

### Reviewed by:

Janko Kos,  
University of Ljubljana, Slovenia  
Reik Löser,  
Helmholtz Association of German  
Research Centres (HZ), Germany

### \*Correspondence:

Ahsan R. Akram  
ahsan.akram@ed.ac.uk

### Specialty section:

This article was submitted to  
Thoracic Oncology,  
a section of the journal  
Frontiers in Oncology

Received: 13 December 2021

Accepted: 07 February 2022

Published: 10 March 2022

### Citation:

Mathieson L, O'Connor RA, Stewart H, Shaw P, Dhaliwal K, Williams GOS, Megia-Fernandez A and Akram AR (2022) Fibroblast Activation Protein Specific Optical Imaging in Non-Small Cell Lung Cancer. *Front. Oncol.* 12:834350. doi: 10.3389/fonc.2022.834350

Fibroblast activation protein (FAP) is a cell surface prolyl-specific serine protease involved in the regulation of extracellular matrix. Whilst expressed at low levels in healthy tissue, upregulation of FAP on fibroblasts can be found in several solid organ malignancies, including non-small cell lung cancer, and chronic inflammatory conditions such as pulmonary fibrosis and rheumatoid arthritis. Their full role remains unclear, but FAP expressing cancer associated fibroblasts (CAFs) have been found to relate to a poor prognosis with worse survival rates in breast, colorectal, pancreatic, and non-small cell lung cancer (NSCLC). Optical imaging using a FAP specific chemical probe, when combined with clinically compatible imaging systems, can provide a readout of FAP activity which could allow disease monitoring, prognostication and potentially stratify therapy. However, to derive a specific signal for FAP any sequence must retain specificity over closely related endopeptidases, such as prolyl endopeptidase (PREP), and be resistant to degradation in areas of active inflammation. We describe the iterative development of a FAP optical reporter sequence which retains FAP specificity, confers resistance to degradation in the presence of activated neutrophil proteases and demonstrates clinical tractability *ex vivo* in NSCLC samples with an imaging platform.

**Keywords:** optical, non-small cell lung carcinoma, imaging, fibroblast, FAP

## INTRODUCTION

Fibroblast activation protein- $\alpha$  (FAP) is a type II transmembrane glycoprotein which is a member of the serine protease family (1). FAP is minimally expressed by fibroblasts in health, but is highly expressed by activated fibroblasts which can be found in the stroma of epithelial tumours (2, 3). Furthermore, there is increasing evidence of the role of FAP in additional fibroproliferative conditions such as idiopathic pulmonary fibrosis, hepatic fibrosis, rheumatoid arthritis and myocardial infarction (4–7). Within tumours, FAP promotes tumour growth by promoting angiogenesis and ECM remodelling (8) and facilitates the progression of tumours by suppressing the anti-cancer immune response (9, 10). High FAP expression is associated with poor survival, high recurrence rates and more advanced stage in several

cancers, including oral squamous cell carcinoma, ovarian cancer, pancreatic ductal adenocarcinoma and non-small cell lung cancer (NSCLC) (11–15). Specifically in NSCLC, FAP expression has been associated with a higher peripheral neutrophil and lymphocyte count ratio and worse overall survival (16).

FAP has both endopeptidase activity (cleaving post proline peptide bonds of non-terminal amino acids) and exopeptidase activity (cleaving peptide bonds of terminal amino acids) (17) and is upregulated *in vitro* by TGF- $\beta$  and IL-1 $\beta$  (18). Closely related peptidases include the dipeptidyl peptidases (DPPs), which have exopeptidase activity, and prolyl endopeptidase [PREP or prolyl oligopeptidase (POP)], which has endopeptidase activity (19). DPP-IV is highly expressed in many tissues (20), and PREP is a closely related peptidase which in the past has been used interchangeably with FAP (21, 22). As PREP has also been found to be present in the membrane of fibroblasts and is distinctive over FAP, selectivity is crucial (23).

Prior studies investigating FAP as an optical probe target focussed on near infrared (NIR) fluorophores where signal can be detected with minimal intrinsic tissue autofluorescence. Li et al. designed an activatable NIR fluorescent probe (ANP<sub>FAP</sub>) for FAP which was composed of the NIR dye Cy5.5 and the quencher dye QSY21 which were linked by a peptide sequence which is cleaved specifically by FAP (KGPGPNQC) (24). In murine tumour models the probe had a higher signal in FAP expressing tumours, but the study did not demonstrate selectivity over PREP. Although not developed as an imaging optical agent for *in vivo* use, Bainbridge et al. describe a FAP specific sequence for assaying circulating FAP, demonstrating a sequence with specificity over PREP (25).

Fluorescent probes are now being used in humans for detection of enzymatic activity in combination with technologies such as optical endomicroscopy (26, 27), and FAP presents an attractive target as there is significant upregulation in NSCLC (28). Optical imaging confers the advantages of a non-ionising source with high resolution imaging with dynamic readouts. When combined with endomicroscopy, this dynamic imaging method could allow for local monitoring of the FAP activity in patients through therapy.

This work aims to develop a FAP specific probe for use in humans with NSCLC that is specific over PREP and DPP-IV, resistant to degradation in areas of active inflammation and compatible with novel endomicroscopy platforms. We demonstrate development of a FAP specific probe that allows for both detection of fluorescence changes and fluorescence lifetime changes in NSCLC *ex vivo*, when used with an optical endomicroscopy platform.

## MATERIALS AND METHODS

### Ethics Statement

Healthy volunteer blood was obtained following informed consent and the study was approved by Lothian Regional Ethics Committee (REC) (REC No: 20-HV-069) prior to enrolment in the studies. Cancer tissue was obtained following

approval by NHS Lothian REC and facilitated by NHS Lothian SAHSC Bioresource (REC No: 15/ES/0094). All participants provided written informed consent. NSCLC tissues lung samples were collected from patients undergoing surgical resection with curative intent.

### Chemical Synthesis

Details of the chemical synthesis are provided in the **Supplementary Methods**.

### Probe Reconstitution

FAP1<sub>Li-FAM</sub> and FAP1D<sub>Li-FAM</sub> were reconstituted in DMSO to a stock solution of 10 mM and aliquots stored at -20°C. Fresh aliquots were reconstituted in the required buffer for each experiment. All other probes were water soluble and were reconstituted to 1 mM in deionised water and stocks frozen at -20°C.

### Recombinant Enzyme Reconstitution

Recombinant human enzymes [rhFAP (R&D Systems), rhPREP (R&D Systems) and rhDPP-IV (Biolegend)] were stored in stocks at -70°C and diluted as required to be used at final concentration of 0.1  $\mu$ g/ml. Enzymes were aliquoted upon receipt from the supplier and new stocks made from a fresh aliquot as required. Stocks were made at [4x] and control substrates of Z-Gly-Pro-AMC and H-Gly-Pro-AMC (Bachem) were used to confirm activity for each new stock of enzyme.

### Assessment With Recombinant Enzymes

Assays were undertaken in triplicate in blackened 384 well plates on ice prior to spectral reads. All solutions were diluted in TRIS buffer (25 nM Tris, 250 nM NaCl, pH 7.5). Probes were used at 5  $\mu$ M and inhibitors (namely Talabostat (also referred to as Val-boroPro), Merck) at 10  $\mu$ M, unless otherwise stated. All wells contained a final volume of 20  $\mu$ l to include buffers, inhibitors (if used), substrates and recombinant human enzymes (at a concentration of 0.1  $\mu$ g/ml unless otherwise stated). This equates to molarity concentrations of 1.16 micromolar for FAP, 1.23 micromolar for PREP and 1.16 micromolar for DPP-IV. Plates were sealed with an optical plate sealer (Biolegend) and were read in a preheated spectrophotometer (Synergy Biotek) in monochromator-based mode at 380/460 nm for control substrates and 480/530 nm for synthesised FAP probes.

### Assessment on Neutrophil Lysate

Neutrophils were isolated from peripheral blood of healthy volunteers by discontinuous percoll gradients, as previously described (29). Cells were resuspended in PBS (at 10 million cells/ml) and stimulated with 1  $\mu$ M calcium ionophore, then lysed with 1% Triton-X-100. Lysate was used at 1:1 dilution for experiments, replacing recombinant enzymes in the assay as described above, with PBS as the buffer.

## Assessment on Cancer Associated Fibroblasts (CAFs)

CAFs were isolated from NSCLC patient samples as previously described (28). Briefly, tissue samples were minced with forceps and incubated for an hour in prewarmed RPMI media (Gibco) containing collagenase IV [2 mg/ml] (Sigma) and DNase [0.2 mg/ml] (Sigma). Samples were spun at 350 g for 5 minutes and red blood cells were lysed from samples using RBC lysis buffer (BioLegend) in 10 ml for 10 minutes. Following a further spin at 350 g for 5 minutes, cells were seeded in culture flasks in DMEM containing 10% FCS, 1% Penicillin-Streptomycin, 1% L-Glutamine and 10% Insulin Transferrin Selenium (ITS). 24 hours after seeding, non-adherent cells were washed from the flasks. Cells were maintained by standard cell culture methods and by passage 2, the predominant cell type was CAFs, assessed by flow cytometry markers and morphology. CAFs between passage 4-9 were used to assess FAP probes and confirmed to be FAP<sup>hi</sup> by flow cytometry.

CAFs were seeded into 96 well plates in a 100  $\mu$ l media (complete DMEM as described above) at a density of  $1 \times 10^5$  cells/ml to form a confluent monolayer within 24 hours. Wells containing cells had media removed and then were washed before buffer (DPBS) +/- inhibitors were added with the imaging probes. Immediately after adding imaging probes, the plate was transferred to the prewarmed spectrophotometer as above and read at 480/530 nm for one hour.

For imaging, CAFs were seeded in glass bottom chambers (Ibidi), grown, and fixed with 4% paraformaldehyde for 20 minutes at 4°C. Following three washes, cells were permeabilised with 0.2% Triton X-100, quenched with ammonia chloride (50mM) for 5 minutes and blocked with 1% BSA. FAP antibody at 1:100 (AF3715, R&D systems) was incubated overnight at 4°C, washed, incubated with secondary antibody (goat anti-sheep) conjugated to Alexa Fluor 633 (1:1000) and Alexa Fluor 488 Phalloidin 5  $\mu$ L/250  $\mu$ L (A12379, Life Technologies) for 1 hour and finally incubated with DAPI (D1306, Life Technologies) in the dark for 5 minutes. Images were taken on Leica SP5 confocal microscope (Leica Microsystems, Wetzlar, Germany) using dedicated laser excitation at 405 nm, 488 nm and 633 nm.

## Flow Cytometry

Cells collected in suspension (CAFs or neutrophils) were stained with a live/dead marker Zombie UV (1:1000, Biolegend) for 30 min at room temperature in DPBS (Gibco). Cells were then washed and stained with an anti-FAP-APC antibody (1:20, R&D Systems) for 20 mins at 4°C in DPBS supplemented with 2% FCS. After washing cells were fixed in a 1:1 solution of fixation buffer (Biolegend) and DPBS with 2% FCS overnight at 4°C before data acquisition on a LSR6Fortessa analyser (BD Biosciences). Flow cytometry data was then analysed using FlowJo version 10.7.1. Compensation was carried out using single stain control UltraComp eBeads (Invitrogen) and isotype control samples were stained using iso-anti-FAP-APC (1:20, R&D Systems). FAP expression was determined by gating on singlet, live cells

and then looking at anti-FAP-APC signal compared to the isotype control.

## Fluorescence and Lifetime Imaging

For imaging solutions, varying concentrations of rhFAP were prepared in blackened eppendorfs and FAP3 to a final concentration of 5  $\mu$ M added and imaged as below. For biological specimens, NSCLC patient tissue samples from surgical resection were used fresh or snap frozen and stored at -80°C until required. Small fragments (approx. 4mm<sup>3</sup>) incubated at 37°C in a 96 well plate in phenyl-red free DMEM (Gibco) containing 10% FCS, 1% Penicillin-streptomycin and 1% L-Glutamine. For the tissue fragments to be used as inhibitor controls, we added Talabostat at a dilution of 1:1000. Samples were then imaged using a clinically approved fluorescence lifetime imaging system used in conjunction with an imaging fibre (30) providing a 400 x 400  $\mu$ m field of view. The imaging system incorporates a pulsed supercontinuum laser source, in this case tuned for excitation at 488 nm, with an achromatic confocal laser scanning system and a time-resolved spectrometer. This spectrometer contains a 512 channel single photon avalanche diode (SPAD) sensor (31) allowing for the rapid collection of time resolved spectral fluorescence lifetime data. Fluorescence intensity and lifetime images were collected using an image resolution of 160 x 160 pixels over a 498 – 570 nm spectral range with an exposure time of 13  $\mu$ s per pixel. This led to an imaging rate of ~3 frames per second.

For each condition, the tumour samples were imaged using a fibre placed at the surface of the tissue (baseline), and then again at 10-minute intervals following the additions of equimolar concentrations of probe +/- Inhibitor. For imaging solutions, the fibre was held within the solution and imaged every 5 minutes. Each condition and time-point data for both fluorescence intensity and lifetime were collected. Imaging sequences had non-relevant frames removed, and the entire field of view was analysed. Analysis was undertaken using a bespoke software suite utilising the rapid lifetime determination (RLD) method (32). The RLD method utilises two-time bins for reduced data load and high-speed analysis whilst retaining reasonable lifetime approximation for single exponential decays. Whilst the sample analyses are likely multi-exponential in character the lightweight RLD algorithm provides a good approximation to the intensity weighted average lifetime observed, providing sufficient discrimination of sample type. Data had background subtraction, lightfield normalisation and an intensity threshold (of 20 counts) applied through all sequences. Intensity data are provided as relative units (RU) and lifetime as nanoseconds (ns).

## RESULTS AND DISCUSSION

### Optimizing Fragment for FAP Specificity

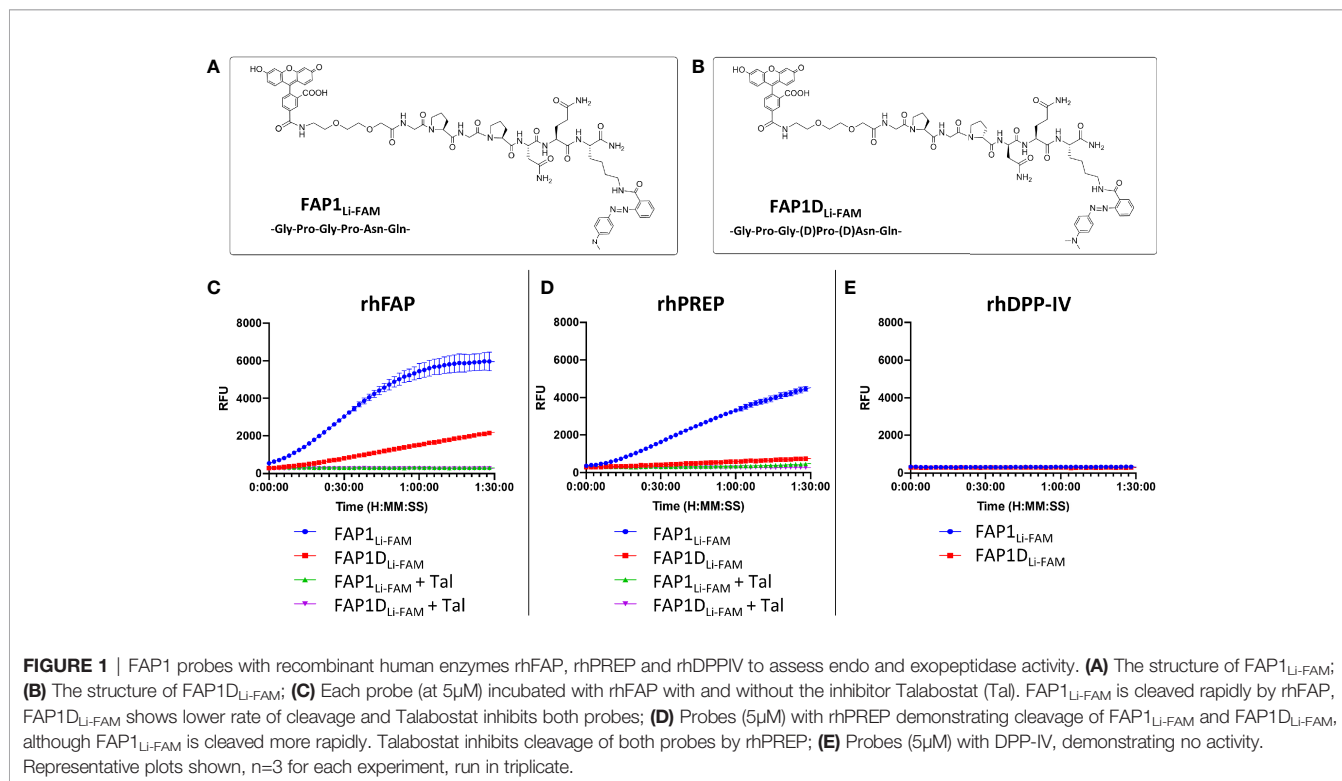
As starting point for our study, a peptide sequence previously published within a FAP optical reporter was synthesised (GPGPNQ), which had been determined to be FAP specific

over DPP-IV but had not been assessed against PREP (24). We synthesised the reported peptide sequence but for FRET pairing we utilised a Carboxyfluorescein (FAM) fluorophore with a Methyl Red quencher (**Figure 1A**) as an alternative to Cy5.5/QSY21. The peptide sequence was synthesized by Fmoc solid-phase peptide synthesis on ChemMatrix resin using Oxyma/DIC as the coupling combination. FAM was incorporated at the N-terminal of the peptide after an ethylglycol unit, and Methyl Red was added at the side chain of a Lys residue at the C-terminal. All probes were purified and characterized by RP-HPLC and MALDI TOF MS (ESI for details). Assessment of this probe (termed FAP1<sub>Li-FAM</sub>) sequence against the recombinant enzymes FAP and PREP demonstrated endopeptidase activity through PREP as well as FAP (**Figures 1C, D**), which was independently demonstrated by Bainbridge et al. (25) for the same sequence. Confirming previous reports, DPP-IV did not cleave the probe (**Figure 1E**) signifying absent exopeptidase activity as the proline residues are not in terminal positions. For inhibition we used Talabostat, also known as Val-boroPro, which is a non-selective inhibitor of dipeptidyl peptidases (DPPs), including DPP-IV, DPP-8, DPP-9, fibroblast activation protein (FAP), and prolyl endopeptidase. The IC<sub>50</sub> (nmol/l) for DPP-IV, FAP and PREP are 4, 390 and 560 respectively (33). Talabostat successfully abrogated the signal (**Figure 1D**).

The construct has Gly-Pro repeats susceptible to PREP cleavage, therefore modifications to block the endopeptidase action by the second proline were made with D-proline and D-asparagine (GPGpnQ) to try and confer a uniquely FAP cleavable probe (FAP1D<sub>Li-FAM</sub> structure shown in **Figure 1B**).

This demonstrated partial reduction in activity in the presence of PREP (**Figure 1D**), but also demonstrated that FAP activity was significantly reduced (**Figure 1C**). Further iterations were assessed against FAP1<sub>Li-FAM</sub> and FAP1D<sub>Li-FAM</sub> activity to assess cleavage efficacy.

Whilst there was an improvement in the specificity, FAP1D<sub>Li-FAM</sub> still demonstrated PREP cleavage so additional compounds were synthesised to overcome this. Shorter versions with modified sequences were synthesised, and the amino acid prior to proline altered in six iterations (structures shown in **Figure 2A**), as it had been previously reported that such modification can introduce FAP specificity (25). At the carboxy-terminus of the peptide, two replicates of bisethyleneglycol and D-lysine were added to ensure both solubility and stability against proteases (34). These six different compounds were then reassessed with recombinant human enzymes (**Figures 2B–D**). Insertion of Ala (FAP2A<sub>Ala</sub>) demonstrated cleavage by PREP and FAP activity was absent, and the insertion of D-Tyr also resulted in loss of FAP activity. The iterations containing D-Ala, D-Ser, D-Thr and β-Ala in the position prior to proline all demonstrated FAP specificity over PREP, however, with reduced signal that may preclude clinical translation. Assessment against DPP-IV confirmed no iterations had introduced exopeptidase activity (**Figure 2D**). As the clinical setting requires rapid optical readout, two further iterations containing D-Ser (FAP3 and FAP-sp) were made inspired by FAP2C<sub>D-Ser</sub> results, which demonstrates FAP specificity (**Figures 2B, C**) without PREP cleavage whilst displaying the strongest signal compared to the other iterations (**Figure 2E**). Comparison with the FAP1<sub>Li-FAM</sub>



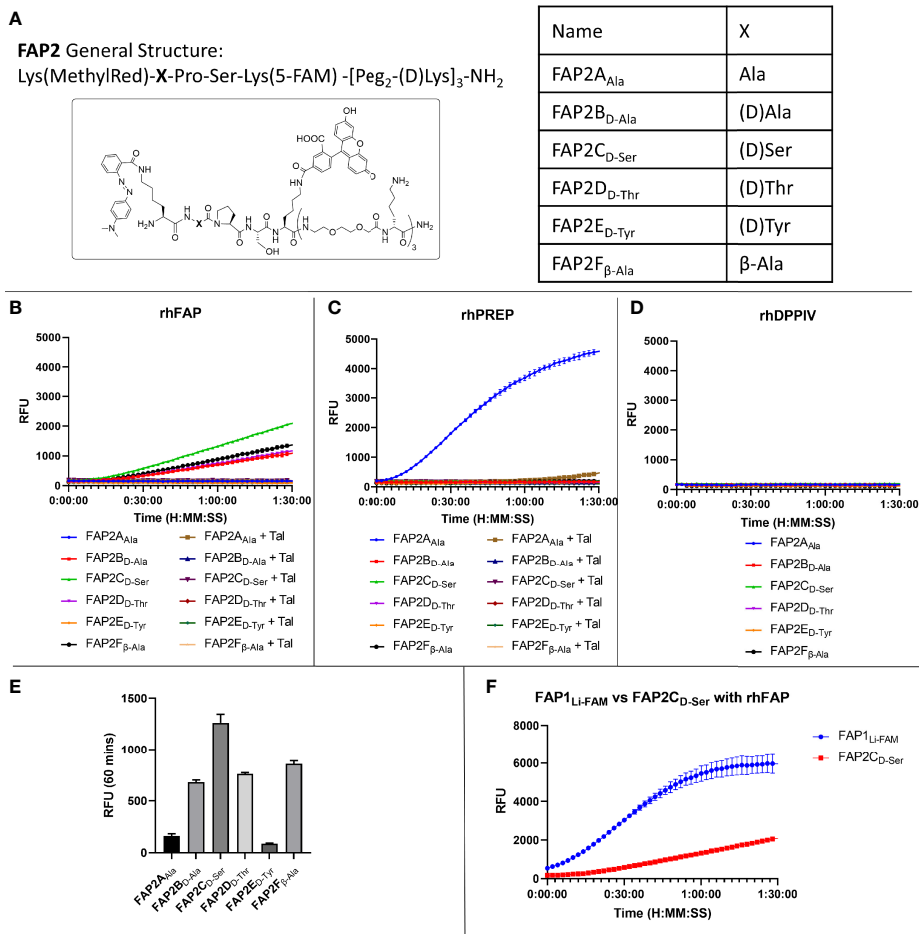


**FIGURE 2** | Iterations of probe FAP2 to determine a sequence specific for FAP over PREP. **(A)** The structure of FAP2 probes and the different variations in the amino acid X; **(B)** Assessment of the probes (5 $\mu$ M) against rhFAP showing relative intensity and Talabostat (Tal) inhibiting cleavage. FAP2C<sub>D-Ser</sub> shows highest rate of cleavage; **(C)** Assessment of the probes (5 $\mu$ M) against rhPREP showing iteration FAP2A<sub>Ala</sub> is cleaved by rhPREP; **(D)** Assessment of the probes against DPP-IV (5 $\mu$ M) showing none of the iterations are cleaved; **(E)** Comparison of the relative fluorescence intensity of each probe iteration at 60 minutes; **(F)** Comparison of FAP1<sub>LI-FAM</sub> with FAP2C<sub>D-Ser</sub> showing the signal intensity of FAP1 is higher within 90 minutes. Representative images, n=3, mean RFU plotted in bar graph and error bars show standard deviation.

compound demonstrated a low signal (**Figure 2F**), and this served as a comparison to additional compounds.

## Improvement of Signal-to-Noise

Using the D-Ser iteration we increased the peptide chain to include Asn to derive a novel sequence (**FAP3**: Lys(MethylRed)-Val-(D)Ser-Pro-Asn-Gln-Gly-Lys(5-FAM)-[Peg<sub>2</sub>-(D)Lys]<sub>3</sub>-NH<sub>2</sub>) or with Ser (**FAP-sP**) and to act as a comparator (structures shown in **Figures 3A, B**). FAP-sP was previously reported by Bainbridge to be utilised as a serum FAP detection probe (25). Both sequences demonstrated FAP specificity (**Figure 3C**) with improved signal characteristics which were further confirmed by MALDI-TOF analysis (**Supplementary Figure S1**). Testing also confirmed no cleavage by PREP or DPP-IV for either compound (**Figures 3D, E**).

## Assessment of Probe in Biological Environments

To assess whether the sequence had sufficient robustness for clinical translation we assessed whether; i) the probe remains intact in areas of low FAP but high protease activity, and ii) the imaging probe can detect physiological levels of FAP. To ensure specificity is maintained in an inflamed environment the probe was assessed against activated neutrophils as these are one of the most predominant leucocyte cell subtypes in cancer (35). Neutrophils were confirmed to be negative for FAP (**Figure 4A**, gating strategy **Supplementary Figure S2**). FAP3 was stable in the presence of neutrophil lysate, however, FAP-sP was cleaved (**Figure 4B**) in a non-FAP dependent manner. Subsequent analysis by MALDI-TOF revealed all FAP-sP probe was cleaved by activated neutrophil lysate, but FAP3 remained intact (**Supplementary Figures S3A, B**). The mechanism

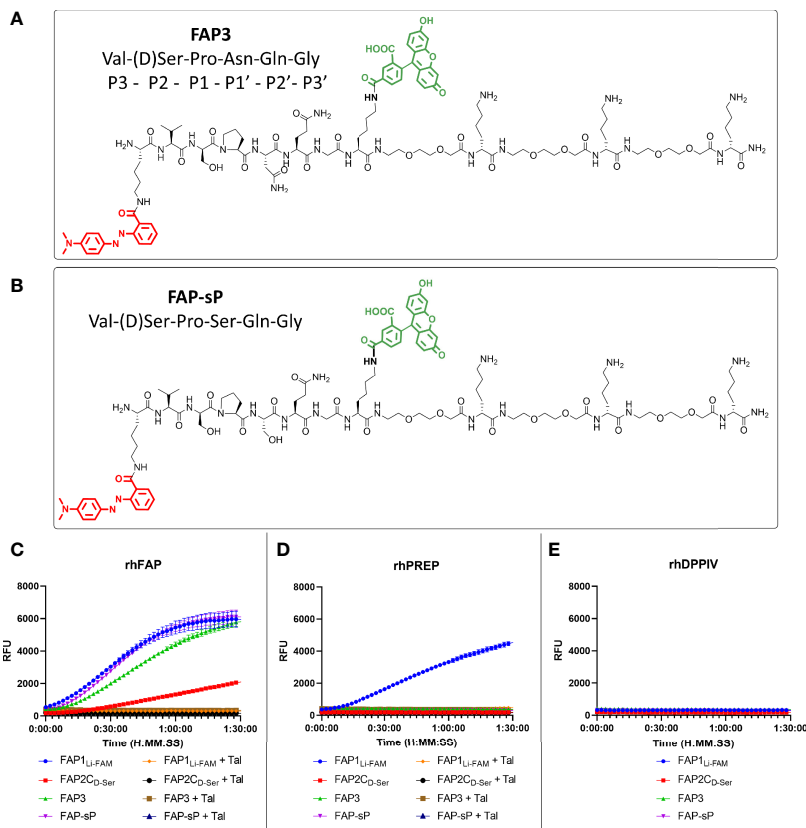


**FIGURE 3** | FAP3 assessment against FAP-sP demonstrates FAP specificity. **(A)** The structure of FAP3; **(B)** The structure of FAP-sP; **(C)** Assessment of FAP3 and FAP-sP (all 5 $\mu$ M) when compared to prior iterations.; **(D)** rhPREP assessment demonstrating no rhPREP cleavage for FAP3 or FAP-sP; **(E)** DPPIV assessment demonstrating no exopeptidase activity. Representative plots, n=3 for each experiment run in triplicate.

causing cleavage/degradation of FAP-sP remains unclear and may include additional proteases from activated neutrophils acting on the substrate, however this provides additional confidence for FAP3 as it remains intact.

Cancer associated fibroblasts were isolated and cultured from NSCLC patient samples (**Figure 4C**) and confirmed to be FAP expressing (**Figure 4D**, gating strategy **Supplementary Figure S4**), in line with our previous work (28). FAP3 was incubated with increasing concentrations of substrate (**Figure 4E**), which demonstrated a  $K_M$  value of 2.168 (SE +/- 0.3736)  $\mu$ M and  $V_{max}$  of 109.5 (SE +/- 7.119) RFU/min. For FAP3 this equates to a  $k_{cat}$  of 0.081236 (+/- 0.005281)  $\text{min}^{-1}$  and a  $k_{cat}/K_M$  ratio of  $3.747 \times 10^4 \text{ M}^{-1} \text{ min}^{-1}$ . FAP3 was cleaved by FAP<sup>+</sup>CAFs, with inhibition of signal when co-incubated with Talabostat (**Figure 4F**). Finally, to ensure stability in the presence of other matrix remodelling proteases found to be upregulated in NSCLC, FAP3 was assessed against a panel of MMP's including MMP 2,9,13 demonstrating no activity (**Figure 4G**). Therefore, FAP3 is a FAP specific sequence over PREP, DPP-IV and MMP's, that can detect FAP within physiological levels and remains resistant to non-specific inflammatory cell degradation.

## Fluorescence Lifetime Imaging (FLIM) of NSCLC Tissue

Label free optical imaging modalities have the potential to characterize lung cancer using both optical endomicroscopy and fluorescence lifetime imaging (FLIM) systems (36). Here we used a clinically approved fluorescence and FLIM imaging system (31) which was compatible with bronchoscopy, where a fibre can be passed through the working channel to access tumours and lung parenchyma (**Supplementary Figure S5**). FLIM imaging utilizes the exponential decay rate of the photon emission from the fluorophores (fluorescence lifetime) to create the image, which provides additional data over fluorescence intensity alone. This system is entering clinical trials and can simultaneously measure fluorescence intensity and lifetime based imagery.

To assess the ability of the system to detect both fluorescence intensity and lifetime changes over time, varying concentrations of rhFAP were incubated with 5 $\mu$ M FAP3 and imaged for up to 40 minutes (**Supplementary Figure S6**). Increases in both fluorescence intensity and lifetime were demonstrated, within 5 minutes, over time showing the capability of the FLIM imaging modality to track changes in these parameters in relevant concentrations and timeframes. As the concentration of rhFAP

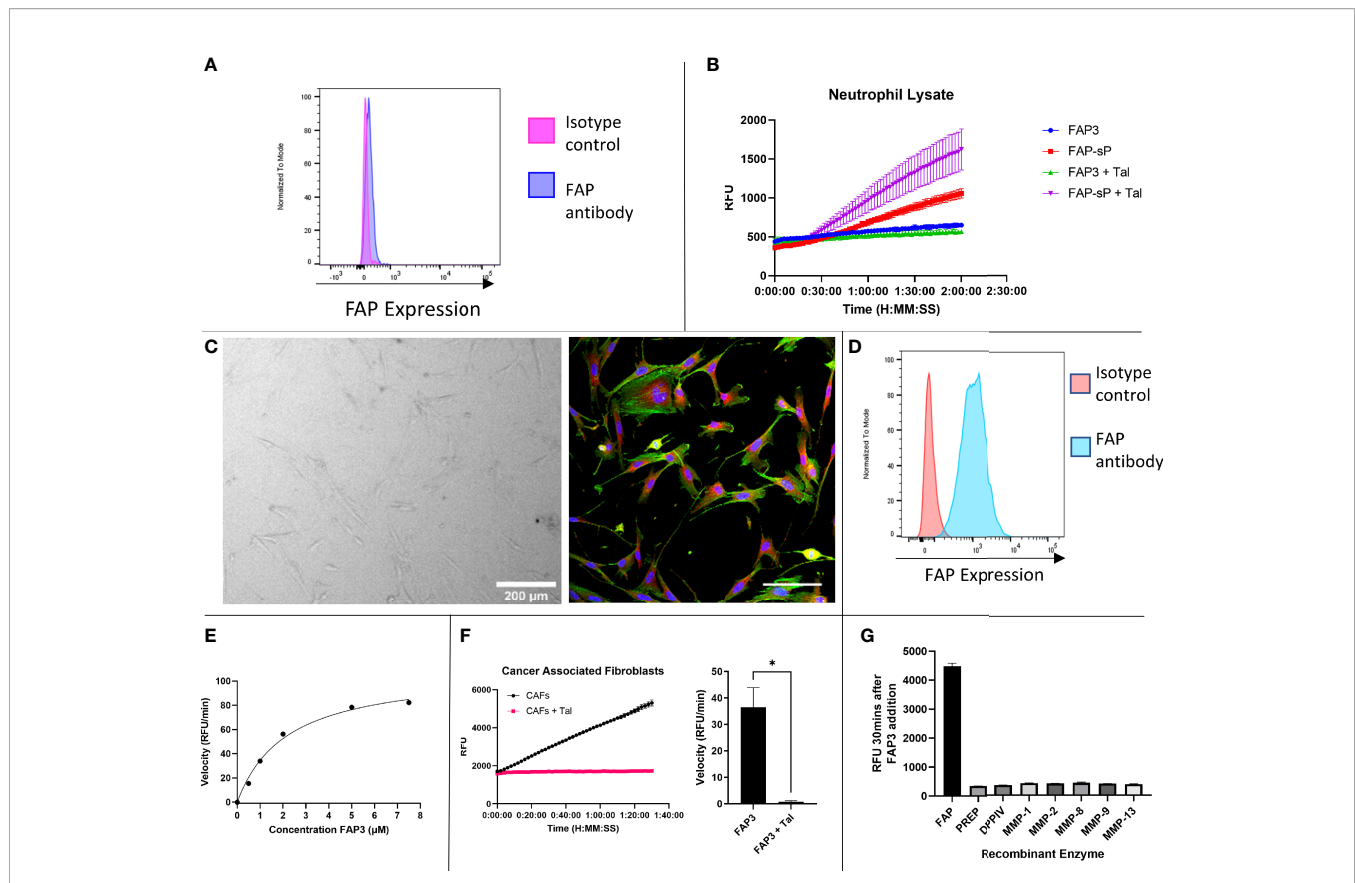


**FIGURE 4** | FAP3 and FAP-sP probes assessed on activated neutrophil lysate and cancer associated fibroblasts (CAFs). **(A)** Flow cytometry confirmed that neutrophils are FAP negative; **(B)** Assessment of FAP3 and FAP-sP in activated neutrophil lysate demonstrated cleavage of FAP-sP, including in the presence of Talabostat (Tal), but no cleavage of FAP3; **(C)** Cancer associated fibroblasts in culture (brightfield, 200µm scale bar) and antibody stained for FAP (red), DAPI (blue) and phalloidin (green), scale bar 100µm; **(D)** Flow cytometry confirmed CAFs are FAP positive; **(E)** Enzyme kinetics of using varying concentrations of substrate FAP3 in presence of rhFAP; **(F)** When incubated with CAFs FAP3 (5µm) was cleaved and signal was abrogated in the presence of Talabostat; representative plot on left and sum of velocity in RFU/min shown on right.; **(G)** FAP3 demonstrates no activity for other recombinant enzymes (MMPs) likely to be present in NSCLC. n=2 for neutrophil lysate testing and MMP testing, n=3 for CAF testing, each experiment run in triplicate. Representative images shown \*p < 0.05.

increased, a corresponding increase in both fluorescence intensity and lifetime was observed.

Next, to assess if using FAP3 we could detect FAP specific cleavage (measured by a change in fluorescence intensity or lifetime) in biological samples we utilized ex vivo lung cancer specimens including two adenocarcinomas, two squamous cell carcinoma and one adenosquamous carcinoma. Representative images showing the intensity and FLIM measurements taken from the imaging system are shown in **Figure 5A** and the change in FLIM and intensity over time for this sample are shown in **Figure 5B**, further showing the increasing signals with time, related to the presence of FAP. All tumours demonstrated a baseline intrinsic autofluorescence signature that was used to track relative changes against the presence of probes (**Supplementary Figure S7**). Across all samples there was an increase in fluorescence intensity and a change to a longer lifetime signature following the addition of FAP3 over time, both of which were abrogated by the inhibitor Talabostat. Summation of the data demonstrated significant FAP dependent increase in both intensity and longer lifetime across all samples (**Figure 5C**). Assessing the data

on a per cancer basis (**Supplementary Figure S7**) there are two interesting features to note - the FLIM signature of the intact probe becomes the dominant signature irrespective of the intrinsic autofluorescence signature and secondly, the rate of change varies amongst the different samples (CR68 and CR126 demonstrate maximum change within 10 minutes). This was most apparent for CR126 where the addition of the probe resulted in demonstration of immediate changes in FLIM ahead of the detectable fluorescence intensity increase for the same sample (**Supplementary Video 1**). Together, this demonstrates FAP3 can detect FAP specific activity in NSCLC using both changes in fluorescence intensity and lifetime and the higher rate of cleavage indicates presence of a higher concentration of FAP. The tracking of these dynamics was made possible by the high acquisition speed of the imaging system.

## CONCLUSIONS

We have developed an optical imaging probe capable of FAP imaging within physiological levels in NSCLC patient derived

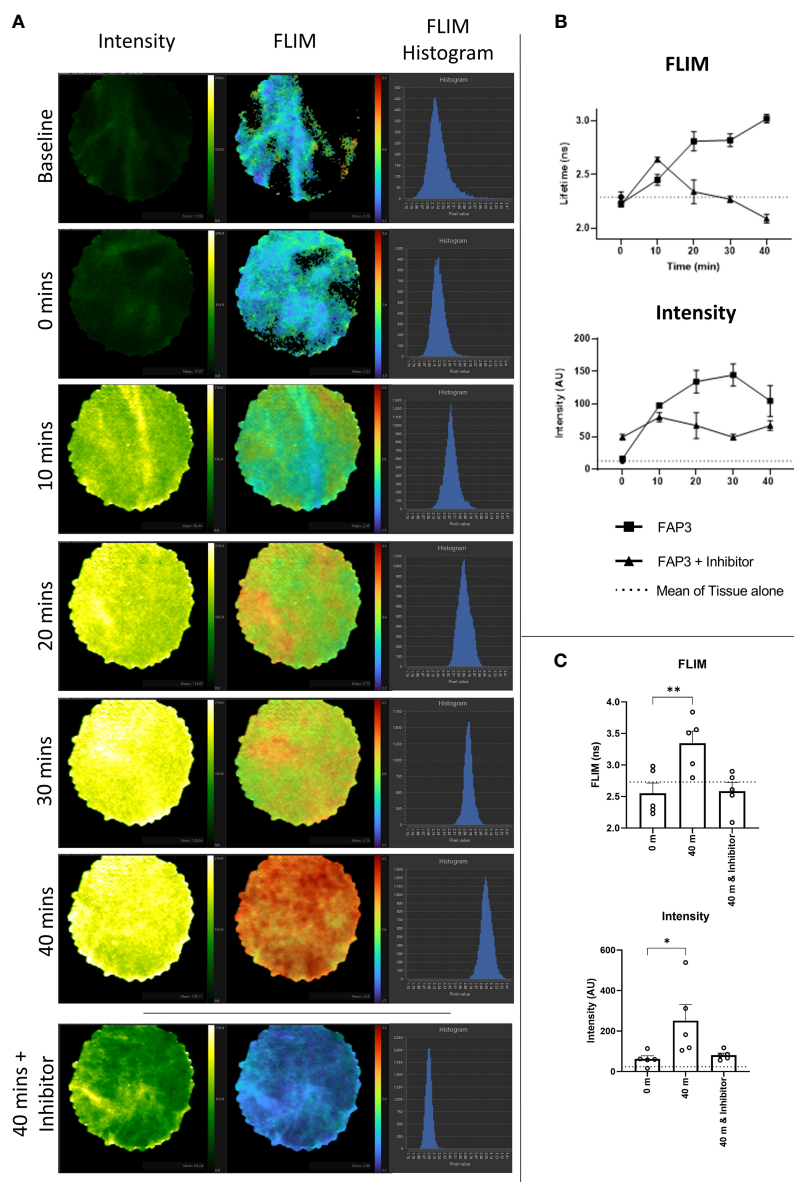


**FIGURE 5** | Fluorescence lifetime imaging in NSCLC tissue using FAP3 probe and a clinically approved FLIM system. **(A)** Representative images showing the change in fluorescence intensity and lifetime after 488nm excitation of a NSCLC tumor tissue sample over time when incubated with FAP3 at 5 $\mu$ M, with lowest panel demonstrating the late time point with presence of the inhibitor Talabostat; **(B)** Representative plots showing the change in intensity and fluorescence lifetime over 40 mins on a NSCLC tissue sample; **(C)** Aggregate analysis across 5 NSCLC samples at 40 minutes demonstrating a significant increase in fluorescence lifetime and intensity, with inhibition in the presence of Talabostat. N=5, analysis by paired t-test, \* $p < 0.05$ , \*\* $p < 0.01$ .

cancer associated fibroblasts and demonstrated changes in fluorescence intensity and lifetime in several patient samples using an imaging system undergoing clinical translation. Furthermore, we have demonstrated specificity over PREP, a closely related endopeptidase to FAP, DPP-IV and MMPs and demonstrated stability in highly proteolytic conditions by testing against activated neutrophils. We have therefore developed a FAP specific optical imaging probe which has potential

applications in imaging of NSCLC as well as other FAP mediated inflammatory conditions.

## DATA AVAILABILITY STATEMENT

The original contributions presented in the study are included in the article/**Supplementary Material**. Further inquiries can be directed to the corresponding author.

## ETHICS STATEMENT

The studies involving human participants were reviewed and approved by Lothian Regional Ethics Committee (REC) (REC No: 20-HV-069) and NHS Lothian REC and facilitated by NHS Lothian SAHSC Bioresource (REC No: 15/ES/0094). The patients/participants provided their written informed consent to participate in this study.

## AUTHOR CONTRIBUTIONS

LM undertook *in vitro* and *ex vivo* experimentation. RO'C undertook supervision and *in vitro* and *ex vivo* experimentation. PS undertook MALDI analysis. AM-F designed and synthesized the probes. HS, KD, and GW developed the FLIM imaging system and analysis methods and supported the clinical translational development of the imaging system and software. AA undertook conception, design of work and supervised the project as well as experimentation. LM and AA wrote the manuscript. All authors approved the manuscript.

## FUNDING

This work was funded by a Cancer Research UK Clinician Scientist Fellowship award to ARA (A24867). LM and PS are

funded through the EPSRC and MRC Centre for Doctoral Training in Optical Medical Imaging (EP/L016559/1). AM-F acknowledges Engineering and Physical Sciences Research Council (EPSRC, United Kingdom, grant number EP/R005257/1).

## ACKNOWLEDGMENTS

The FLIM system and clinical software development was through a EPSRC funded Healthcare Impact Partnership project (EP/S025987/1), CARB-X award (Award Number 4500003353) and EP/LO16559/1. We are grateful for assistance from CIR Flow Cytometry and Shared University Research Facilities, University of Edinburgh.

## SUPPLEMENTARY MATERIAL

The Supplementary Material for this article can be found online at: <https://www.frontiersin.org/articles/10.3389/fonc.2022.834350/full#supplementary-material>

## REFERENCES

- Liu R, Li H, Liu L, Yu J, Ren X. Fibroblast Activation Protein. *Cancer Biol Ther* (2012) 13(3):123–9. doi: 10.4161/cbt.13.3.18696
- Kilvaer TK, Rakaee M, Hellevik T, Østman A, Strell C, Bremnes RM, et al. Tissue Analyses Reveal a Potential Immune-Adjuvant Function of FAP-1 Positive Fibroblasts in Non-Small Cell Lung Cancer. *PLoS One* (2018) 13:1–17. doi: 10.1371/journal.pone.0192157
- Dolznic H, Schweifer N, Puri C, Kraut N, Rettig WJ, Kerjaschki D, et al. Characterization of Cancer Stroma Markers: In Silico Analysis of an mRNA Expression Database for Fibroblast Activation Protein and Endosialin. *Cancer Immun* (2005) 5:1–9.
- Acharya PS, Zukas A, Chandan V, Katzenstein A-LA, Puré E. Fibroblast Activation Protein: A Serine Protease Expressed at the Remodeling Interface in Idiopathic Pulmonary Fibrosis. *Hum Pathol* (2006) 37:352–60. doi: 10.1016/j.humpath.2005.11.020
- Lay AJ, Zhang HE, McCaughan GW, Gorrell MD. Fibroblast Activation Protein in Liver Fibrosis. *Front Biosci (Landmark Ed)* (2019) 24:1–17. doi: 10.2741/4706
- Bauer S, Jendro MC, Wadle A, Kleber S, Stenner F, Dinser R, et al. Fibroblast Activation Protein Is Expressed by Rheumatoid Myofibroblast-Like Synoviocytes. *Arthritis Res Ther* (2006) 8(6):R171. doi: 10.1186/ar2080
- Tillmanns J, Hoffmann D, Habbaba Y, Schmitto JD, Sedding D, Fraccarollo D, et al. Fibroblast Activation Protein Alpha Expression Identifies Activated Fibroblasts After Myocardial Infarction. *J Mol Cell Cardiol* (2015) 87:194–203. doi: 10.1016/j.yjmcc.2015.08.016
- Cheng JD, Dunbrack RL Jr, Valianou M, Rogatko A, Alpaugh RK, Weiner LM. Promotion of Tumor Growth by Murine Fibroblast Activation Protein, a Serine Protease, in an Animal Model. *Cancer Res* (2002) 62:4767–72.
- Joyce JA, Fearon DT. T Cell Exclusion, Immune Privilege, and the Tumor Microenvironment. *Science* (2015) 348(6230):74–80. doi: 10.1126/science.aaa6204
- Kraman M, Bambrough PJ, Arnold JN, Roberts EW, Magiera L, Jones JO, et al. Suppression of Antitumor Immunity by Stromal Cells Expressing Fibroblast Activation Protein-Alpha. *Science* (2010) 330(6005):827–30. doi: 10.1126/science.1195300
- Wang H, Wu Q, Liu Z, Luo X, Fan Y, Liu Y, et al. Downregulation of FAP Suppresses Cell Proliferation and Metastasis Through PTEN/PI3K/AKT and Ras-ERK Signaling in Oral Squamous Cell Carcinoma. *Cell Death Dis* (2014) 5(4):1–11. doi: 10.1038/cddis.2014.122
- Mhaweck-Fauceglia P, Yan L, Sharifian M, Ren X, Liu S, Kim G, et al. Stromal Expression of Fibroblast Activation Protein Alpha (FAP) Predicts Platinum Resistance and Shorter Recurrence in Patients With Epithelial Ovarian Cancer. *Cancer Microenviron* (2015) 8(1):23–31. doi: 10.1007/s12307-014-0153-7
- Shi M, Yu DH, Chen Y, Zhao CY, Zhang J, Liu QH, et al. Expression of Fibroblast Activation Protein in Human Pancreatic Adenocarcinoma and Its Clinicopathological Significance. *World J Gastroenterol* (2012) 18(8):840–6. doi: 10.3748/wjg.v18.i8.840
- Kilvaer TK, Khanekhenari MR, Hellevik T, Al-Saad S, Paulsen E-E, Bremnes RM, et al. Cancer Associated Fibroblasts in Stage I-III NSCLC: Prognostic Impact and Their Correlations With Tumor Molecular Markers. *PLoS One* (2015) 10(8):e0134965. doi: 10.1371/journal.pone.0134965
- Puré E, Blomberg R. Pro-Tumorigenic Roles of Fibroblast Activation Protein in Cancer: Back to the Basics. *Oncogene* (2018) 37(32):4343–57. doi: 10.1038/s41388-018-0275-3
- Liao Y, Ni Y, He R, Liu W, Du J. Clinical Implications of Fibroblast Activation Protein-Alpha in Non-Small Cell Lung Cancer After Curative Resection: A New Predictor for Prognosis. *J Cancer Res Clin Oncol* (2013) 139(9):1523–8. doi: 10.1007/s00432-013-1471-8
- Hamson EJ, Keane FM, Tholen S, Schilling O, Gorrell MD. Understanding Fibroblast Activation Protein (FAP): Substrates, Activities, Expression and Targeting for Cancer Therapy. *Proteomics Clin Appl* (2014) 8(5–6, SI):454–63. doi: 10.1002/prca.201300095
- Chung KM, Hsu SC, Chu YR, Lin MY, Jiaang WT, Chen RH, et al. Fibroblast Activation Protein (FAP) Is Essential for the Migration of Bone Marrow Mesenchymal Stem Cells Through RhoA Activation. *PLoS One* (2014) 9(2):1–11. doi: 10.1371/journal.pone.0088772
- Poplawski SE, Lai JH, Li Y, Jin Z, Liu Y, Wu W, et al. Identification of Selective and Potent Inhibitors of Fibroblast Activation Protein and Prolyl Oligopeptidase. *J Med Chem* (2013) 56(9):3467–77. doi: 10.1021/jm400351a
- Loktev A, Lindner T, Mier W, Debus J, Altmann A, Jaeger D, et al. A Tumor-Imaging Method Targeting Cancer-Associated Fibroblasts. *J Nucl Med* (2018) 59(9):1423–9. doi: 10.2967/jnumed.118.210435

21. Larrinaga G, Perez I, Blanco L, López JI, Andrés L, Etxezarraga C, et al. Increased Prolyl Endopeptidase Activity in Human Neoplasia. *Regul Pept* (2010) 163(1):102–6. doi: 10.1016/j.regpep.2010.03.012
22. Ryabtsova O, Jansen K, Van Goethem S, Joossens J, Cheng JD, Lambier A-M, et al. Acylated Gly-(2-Cyano)Pyrrolidines as Inhibitors of Fibroblast Activation Protein (FAP) and the Issue of FAP/prolyl Oligopeptidase (PREP)-Selectivity. *Bioorg Med Chem Lett* (2012) 22(10):3412–7. doi: 10.1016/j.bmcl.2012.03.107
23. Christiansen VJ, Jackson KW, Lee KN, Downs TD, McKee PA. Targeting Inhibition of Fibroblast Activation Protein- $\alpha$  and Prolyl Oligopeptidase Activities on Cells Common to Metastatic Tumor Microenvironments. *Neoplasia* (2013) 15(4):348–58. doi: 10.1593/neo.121850
24. Li J, Chen K, Liu H, Cheng K, Yang M, Zhang J, et al. An Activatable Near Infrared Fluorescent Probe for *In Vivo* Imaging of Fibroblast Activation Protein-Alpha. *Bioconjug Chem* (2013) 23(8):1704–11. doi: 10.1021/bc300278r.An
25. Bainbridge TW, Dunshee DR, Kljavin NM, Skelton NJ, Sonoda J, Ernst JA. Selective Homogeneous Assay for Circulating Endopeptidase Fibroblast Activation Protein (FAP). *Sci Rep* (2017) 7(1):1–12. doi: 10.1038/s41598-017-12900-8
26. Pirovano G, Roberts S, Kossatz S, Reiner T. Optical Imaging Modalities: Principles and Applications in Preclinical Research and Clinical Settings. *J Nucl Med* (2020) 61(10):1419–27. doi: 10.2967/jnumed.119.238279
27. Megia-Fernandez A, Marshall A, Akram AR, Mills B, Chankeshwara SV, Scholefield E, et al. Optical Detection of Distal Lung Enzyme Activity in Human Inflammatory Lung Disease. *BME Front* (2021) 2021:1–11. doi: 10.34133/2021/9834163
28. O'Connor RA, Chauhan V, Mathieson L, Titmarsh H, Koppensteiner L, Young I, et al. T Cells Drive Negative Feedback Mechanisms in Cancer Associated Fibroblasts, Promoting Expression of Co-Inhibitory Ligands, CD73 and IL-27 in Non-Small Cell Lung Cancer. *Oncoimmunology* (2021) 10(1):1940675. doi: 10.1080/2162402X.2021.1940675
29. Haslett C, Guthrie LA, Kopaniak MM, Johnston RB, Henson PM. Modulation of Multiple Neutrophil Functions by Preparative Methods or Trace Concentrations of Bacterial Lipopolysaccharide. *Am J Pathol* (1985) 119(1):101–10.
30. Stone JM, Wood HAC, Harrington K, Birks TA. Low Index Contrast Imaging Fibers. *Opt Lett* (2017) 42(8):1484. doi: 10.1364/ol.42.001484
31. Williams GOS, Williams E, Finlayson N, Erdogan AT, Wang Q, Fernandes S, et al. Full Spectrum Fluorescence Lifetime Imaging With 0.5 Nm Spectral and 50 Ps Temporal Resolution. *Nat Commun* (2021) 12(1):1–9. doi: 10.1038/s41467-021-26837-0
32. Moore C, Chan SP, Demas JN, DeGraff BA. Comparison of Methods for Rapid Evaluation of Lifetimes of Exponential Decays. *Appl Spectrosc* (2004) 58(5):603–7. doi: 10.1366/000370204774103444
33. Lankas GR, Leiting B, Roy RS, Eiermann GJ, Beconi MG, Biftu T, et al. Dipeptidyl Peptidase IV Inhibition for the Treatment of Type 2 Diabetes: Potential Importance of Selectivity Over Dipeptidyl Peptidases 8 and 9. *Diabetes* (2005) 54(10):2988–94. doi: 10.2337/diabetes.54.10.2988
34. Megia-Fernandez A, Mills B, Michels C, Chankeshwara SV, Krstajić N, Haslett C, et al. Bimodal Fluorogenic Sensing of Matrix Proteolytic Signatures in Lung Cancer. *Org Biomol Chem* (2018) 16(43):8056–63. doi: 10.1039/c8ob01790e
35. Kargl J, Busch SE, Yang GHY, Kim KH, Hanke ML, Metz HE, et al. Neutrophils Dominate the Immune Cell Composition in Non-Small Cell Lung Cancer. *Nat Commun* (2017) 8:1–11. doi: 10.1038/ncomms14381
36. Fernandes S, Williams G, Williams E, Ehrlich K, Stone J, Finlayson N, et al. Solitary Pulmonary Nodule Imaging Approaches and the Role of Optical Fibre-Based Technologies. *Eur Respir J* (2021) 57(3):2002537. doi: 10.1183/13993003.02537-2020

**Conflict of Interest:** LM, AMF and ARA are named on a patent relating to the probe construct, filed by The University of Edinburgh. GOSW is named on a patent filed by The University of Edinburgh related to the imaging system.

The remaining authors declare that the research was conducted in the absence of any commercial or financial relationships that could be construed as a potential conflict of interest.

**Publisher's Note:** All claims expressed in this article are solely those of the authors and do not necessarily represent those of their affiliated organizations, or those of the publisher, the editors and the reviewers. Any product that may be evaluated in this article, or claim that may be made by its manufacturer, is not guaranteed or endorsed by the publisher.

Copyright © 2022 Mathieson, O'Connor, Stewart, Shaw, Dhaliwal, Williams, Megia-Fernandez and Akram. This is an open-access article distributed under the terms of the Creative Commons Attribution License (CC BY). The use, distribution or reproduction in other forums is permitted, provided the original author(s) and the copyright owner(s) are credited and that the original publication in this journal is cited, in accordance with accepted academic practice. No use, distribution or reproduction is permitted which does not comply with these terms.